



DOI: 10.34910/MCE.103.9

## The behavior of CFRP strengthened RC beams subjected to blast loading

A. Jahami<sup>a\*</sup>, Y. Temsah<sup>a</sup>, J. Khatib<sup>a</sup>, O. Baalbaki<sup>a</sup>, S. Kenai<sup>b</sup>

<sup>a</sup> Beirut Arab University, Beirut, Lebanon

<sup>b</sup> University of Blida, Blida, Algeria

\* E-mail: [ahjahamy@hotmail.com](mailto:ahjahamy@hotmail.com)

**Keywords:** blast loading, CFRP sheets, deflection, dynamic analysis, impact damage, strengthening

**Abstract.** Carbon Fiber Reinforced Polymer (CFRP) sheets have been widely used in strengthening different concrete elements such as beams, slabs, and columns. This sparked the interest of many researchers to conduct research on CFRP sheets; to have a better understanding for their behavior. This paper studied numerically the effect of using CFRP as a strengthening technique for Reinforced Concrete (RC) beams subjected to blast loading. A previous experimental investigation done by a Chinese researchers was considered in this study as a reference, and was modeled numerically (using ABAQUS) for this study. The model was then calibrated in order to conduct the numerical analysis on the effect of CFRP. Three different configurations of CFRP were considered: bottom CFRP strips for flexural strengthening, diagonal side strips for shear strengthening, and U-shaped strips for both shear and flexural strengthening. The variables considered in this study were; the mid-span deflection, strain in steel reinforcement and structural damage in both beams and CFRP sheets. Results showed that using CFRP in the bottom tensile face of RC beams helps in absorbing blast energy. In addition, using CFRP has shown a reduction in the tensile strain of the beam reinforcements.

### 1. Introduction

Temsah [1, 2] and Jahami [3] have studied numerically the effect of impact loads due to close explosions on the behavior of reinforced concrete beams. The effect of impact loading condition on both concrete and steel reinforcement material properties was considered. It was found that reinforced concrete beams failed locally due to plastic hinge formation. A spalling of concrete was realized at the tension zone in addition to the crushing of concrete at the compression zone. In addition, Iso – damage curves were derived for all beams considered in the study. Other researchers studied numerically the behavior of structural element when subjected to direct impact due to falling objects. These studies included impact of falling object on reinforced concrete beams [4, 5], and on post-tensioned slabs [6–8]. The behavior of these structural elements and its modes of failure were presented. It was shown that a local failure occurred in both studies: a plastic hinge occurred in the reinforced concrete beam, and a punching shear failure occurred in the posttensioned slab at the position of the falling object.

Many researchers [9–13] studied the usage of Carbon fiber Reinforced Polymers (CFRP) sheets in strengthening reinforced concrete beams. Kishore [14] investigated the effect of using CFRP sheets on the flexural and shear capacity of RC beams. The main variables considered in this study were the reinforcement ratio (flexural and shear) and the position of CFRP sheets. Results indicated that beams strengthened by CFRP laminates were structurally efficient. It was concluded that using CFRP sheets increases the flexural and shear capacity of RC beams by 40 % and 45 % respectively.

Other researchers investigated the behavior of RC beams strengthened with CFRP under impact loading conditions [15–19]. Fujikake [20] examined the impact responses of CFRP strengthened reinforced concrete (RC) beams experimentally. The studied parameters were; the height of the falling object, the number of blows, and the CFRP scheme. Four different types of CFRP strengthening schemes were applied to RC beams. This experimental study proved that RC beams strengthened with CFRP have better

Jahami, A., Temsah, Y., Khatib, J., Baalbaki, O., Kenai, S. The behavior of CFRP strengthened RC beams subjected to blast loading. Magazine of Civil Engineering. 2021. 103(3). Article No. 10309. DOI: 10.34910/MCE.103.9



This work is licensed under a CC BY-NC 4.0

resistance to impact loadings. In addition, by strengthening RC beams with CFRP in flexure, crack width was decreased compared to unstrengthened RC beams.

Some studies regarding strengthening techniques for posttensioned slabs subjected to punching shear failure due to direct impact load from a falling object were done. One of them studied the efficiency of using Carbon fiber reinforced polymers "CFRP" to reduce punching shear damage in posttensioned slabs due to impact loads [21]. It was found that using CFRP reduced the mid-span displacement of reinforced concrete slabs when subjected to impact loads. A drop between 15% to 30% was obtained when using this strengthening technique. In addition, more energy was dissipated using CFRP as internal energy. The CFRP sheets proved to be good in absorbing impacts and energy from different loads. It reduced the tensile damage occurred in concrete due to the increase in energy absorption. Similar studies were performed for the same strengthening technique and reached the same conclusions [22, 23].

This work demonstrates the efficiency of using different CFRP sheet configurations on the structural behavior of reinforced concrete beams subjected to blast loading. Both flexural and shear stresses and strains were checked due to different configurations. Also the damage at both top and bottom faces were checked too.

## 2. Methods

### 2.1. Experimental data

The input data used in this numerical study were obtained from the experimental work done by Zhang [24] at National University of Defense Technology. The beams studied in this work had dimensions of 85 cm×7.5 cm×7.5 cm, 110 cm×10 cm×10 cm, and 135 cm×12.5 cm×12.5 cm. However, in this numerical study, the beams with dimensions 110 cm×10 cm×10 cm were considered. All steel reinforcements have diameter of 6 mm as shown in Fig. 1. Four different explosive weights were considered, each was placed over the center of the reinforced concrete (RC) beam. A steel frame was used to support the reinforced concrete beam. The experimental setup and details are shown in Fig. 1, while the experimental program is summarized in Table 1. As for material strength, the concrete compressive strength was 40 MPa, while the steel yield and ultimate strength were 395 MPa and 501 MPa respectively.

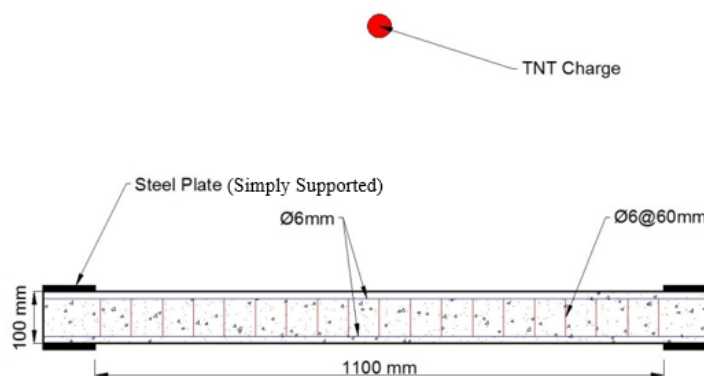


Figure 1. Experimental setup [24].

Table 1. Number and Dimensions of beams.

Beam	Dimensions (mm)	TNT (Kg)	Standoff distance (m)
B2-1	100×100×1100	0.36	0.4
B2-2		0.45	0.4
B2-3		0.51	0.4
B2-4		0.75	0.4

### 2.2. Numerical Modeling

As indicated earlier that the data used in the computer simulation were those of Zhang's experiment [24]. The software used for this purpose was "ABAQUS". The concrete body and steel supports were modelled as solid elements (C3D8R), whereas steel rebars were modelled as wire elements (T3D2) as shown in Fig. 2 and 3 [25]. As for blast loading, ABAQUS built-in model "CONWEP" was used to simulate the explosion, and that was achieved easily by assigning an equivalent TNT explosive to a reference point set at a distance from the target.

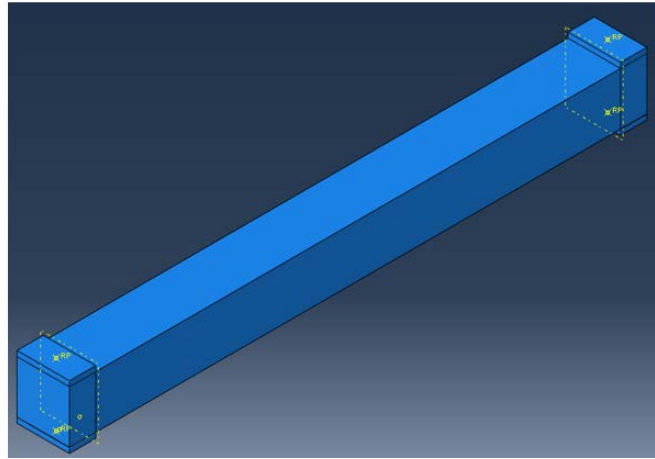


Figure 2. 3D view of beam modelled in ABAQUS.

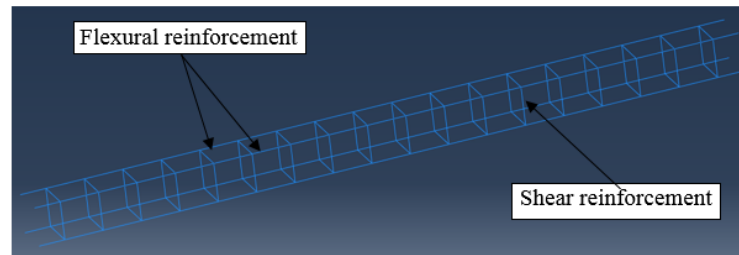


Figure 3. Flexural and Shear reinforcement modelling.

The Concrete Damage Plasticity (CDP) model was used to define the mechanical properties of concrete. This model was derived by Lubliner [26] and developed by Lee [27]. CDP model represents the nonlinear behaviour of concrete using different input parameters like inelastic strain, cracking strain, stiffness degradation and recovery, and other parameters. In addition, the effect of dynamic load conditions on concrete properties was included as per the study done by Jahami [3]. Equations 1 to 5 show the formulas used to determine the dynamic properties of concrete:

$$\frac{f_{cd}}{f_{cm}} = \left( \frac{\varepsilon'_c}{30 \times 10^{-6}} \right)^{\left( \frac{1.016}{5+0.9 f_{cm}} \right)} \quad (1)$$

$$\frac{f_{ctd}}{f_{ctm}} = \left( \frac{\varepsilon'_{ct}}{10^{-6}} \right)^{\left( \frac{1}{1+0.8 f_{cm}} \right)} \quad (2)$$

$$\frac{E_{cd}}{E_{cm}} = \left( \frac{\varepsilon'_c}{30 \times 10^{-6}} \right)^{0.026} \quad (3)$$

$$\frac{E_{ctd}}{E_{ctm}} = \left( \frac{\varepsilon'_{ct}}{3 \times 10^{-6}} \right)^{0.026} \quad (4)$$

$$\frac{\varepsilon_{cd}}{\varepsilon_{cm}} = \left( \frac{\varepsilon'_c}{30 \times 10^{-6}} \right)^{0.02} \quad (5)$$

Where “ $\varepsilon'_c$ ” is the compressive strain rate in concrete, “ $f_{cm}$ ” is the static compressive strength of concrete, “ $f_{cd}$ ” is the dynamic compressive strength of concrete, “ $\varepsilon'_{ct}$ ” is the tensile strain rate in concrete, “ $f_{ctm}$ ” is the static tensile strength of concrete, “ $f_{ctd}$ ” is the dynamic tensile strength of concrete, “ $E_{cm}$ ” is the static elastic modulus of concrete in compression, “ $E_{cd}$ ” is the dynamic elastic modulus of concrete in compression, “ $E_{ctm}$ ” is the static elastic modulus of concrete in tension, “ $E_{ctd}$ ” is the dynamic elastic modulus of concrete in tension, “ $\varepsilon_{cm}$ ” is the static compressive strain at maximum compressive stress, and “ $\varepsilon_{cd}$ ” is the dynamic strain at maximum compressive stress. Concrete mechanical properties for both static and dynamic load conditions are shown below in Table 2:

**Table 2. Mechanical Properties of Concrete.**

Parameter	Notation	Static Condition	Dynamic condition
Elastic Modulus (MPa)	$E$	29725	46341
Poisson's ratio	$\nu$	0.2	0.2
Density (Kg/m <sup>3</sup> )	$\rho$	2400	2400
Compressive strength (MPa)	$f'_c$	40	56.8
Peak Compressive strain (mm/m)	$\epsilon'_c$	2.3	3.2
Tensile Strength (MPa)	$f_t$	3.86	5.48
Dilation angle (°)	$\psi$	36	36
Eccentricity	$\epsilon$	0.1	0.1
Bi-axial to Uni-axial strength ratio	$f_{b0}/f_{t0}$	1.16	1.16
Second stress invariant ratio	$K$	0.67	0.67
Viscosity parameter	$\mu$	0	0

As for the reinforcing steel, the Elasto-Plastic behaviour was implemented in this study [3], and a perfect bond was considered between the rebars and the surrounding concrete. Regarding the contact between the steel supports and the concrete slab, a frictional coefficient of 0.7 was considered. Equations 6 and 7 were used to determine the dynamic yield and ultimate strength of steel rebars.

$$\frac{f_{yd}}{f_y} = \left( \frac{\epsilon'_s}{10^{-4}} \right)^{\left( 0.074 - 0.04 \frac{f_y}{414} \right)} \quad (6)$$

$$\frac{f_{ud}}{f_u} = \left( \frac{\epsilon'_s}{10^{-4}} \right)^{\left( 0.019 - 0.009 \frac{f_y}{414} \right)} \quad (7)$$

Where " $\epsilon'_s$ " is the strain rate in steel, " $f_y$ " is the static yield strength of steel, and " $f_{yd}$ " is the dynamic yield strength of steel. " $f_u$ " is the static ultimate strength of steel, and " $f_{ud}$ " is the dynamic ultimate strength of steel. The steel material property details used in this study are illustrated in Table 3.

**Table 3. Mechanical Properties of Steel reinforcement.**

Parameter	Notation	Static Condition	Dynamic condition
Elastic Modulus (MPa)	$E$	200000	200000
Poisson's ratio	$\nu$	0.3	0.3
Density (Kg/m <sup>3</sup> )	$\rho$	7850	7850
Yield strength (MPa)	$f_y$	395	590
Ultimate strength (MPa)	$f_u$	501	620

### 2.3. Model Calibration

The numerical model was successfully validated and matched with the experimental work. Table 4 represents the mid-span deflection results. All cases were validated with an average error of 6 %. Mid-span deflection curves due to numerical modeling for all beams are shown in Fig. 4. The peak deflection was increased as the blast intensity increased.

**Table 4. Mid-Span Deflection for experimental, SDOF, and Finite element modeling analysis.**

Beam	TNT (Kg)	Standoff distance (m)	Mid-Span Deflection (mm)		Error (%)
			Experimental	ABAQUS	
B2-1	0.36	0.4	9	8.8	2.22
B2-2	0.45	0.4	25	23.5	6
B2-3	0.51	0.4	35	32.1	8.29
B2-4	0.75	0.4	40	36.3	9.25

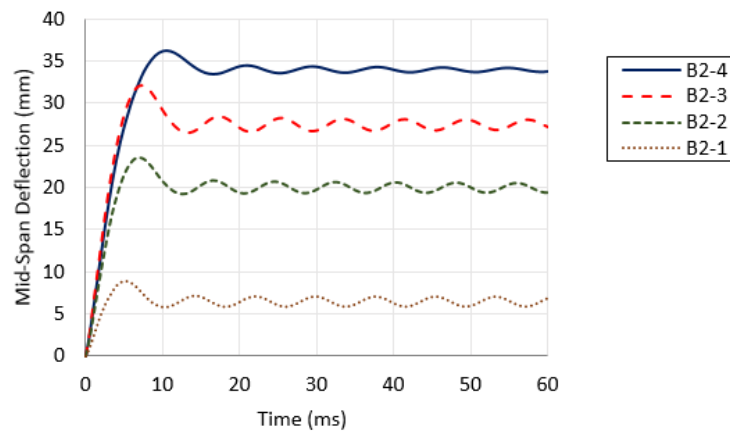


**Figure 4. Mid-Span Deflection (ABAQUS Results).**

The width of both tensile and compressive damage zones was also considered in the validation process. Table 5 shows the damage zone width for both experimental and numerical modeling. Fig. 5 to 8 show the damage extent for beams B2-2 and B2-4 due to blast loading, both at bottom (tension) and top (compression) face. For both beams, the damaged area in compression is larger than that in tension.

**Table 5. Top and Bottom Damage.**

Beam Sample	Compression Fracture Zone Width (cm)			Tensile Fracture Zone Width (cm)		
	Experiment	ABAQUS	Error %	Experiment	ABAQUS	Error %
B2-1	0	0	0	0	0	0
B2-2	8	6	25	7	5.9	15.8
B2-3	10	9	10	12	10.8	10.4
B2-4	12	10.3	14.6	15	13.8	8.3

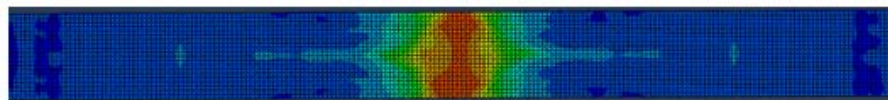


**Figure 5. Compression Damage (B2-2).**

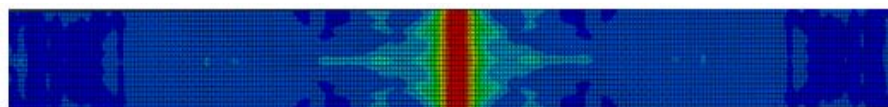


**Figure 6. Tensile Damage (B2-2).**

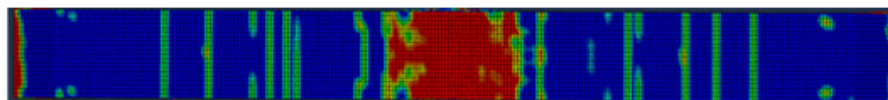


**Figure 7. Compression Damage (B2-4).**

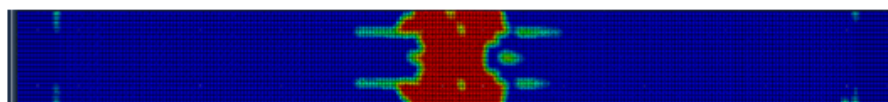


**Figure 8. Tensile Damage (B2-4).**

#### 2.4. Strengthening Plan

After calibration, beam (B2-2) was studied numerically in order to check the efficiency of different applications of CFRP sheets on the mentioned beam. Four cases were considered. The first case was the beam (B0) which represent the beam (B2-2) without any strengthening. The second case was the beam (B1) which was strengthened by 2 bottom strips of CFRP each with 3.5 cm width and 90 cm length. Both strips were placed in a symmetric way as shown in Figure 9. The third case was the beam (B2) which was

strengthened with U-shape strips each with a width of 5 cm as shown in Fig. 10. Finally, the fourth case was the beam (B3) that was strengthened by diagonal strips each with 5 cm width as can be seen from Fig. 11. The properties of the used CFRP are illustrated in Table 6:

**Table 6. Mechanical properties of CFRP sheets used strengthening.**

Parameter	Notation	Value
Modulus of Elasticity	$E$	74.7 GPa
Tensile strength	$F_t$	933 MPa
Maximum strain	$\epsilon_t$	1.25%

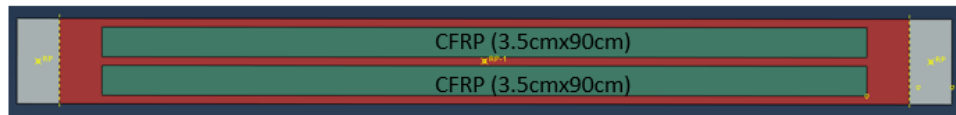


**Figure 9. The bottom face of beam (B1) strengthened with bottom strips.**

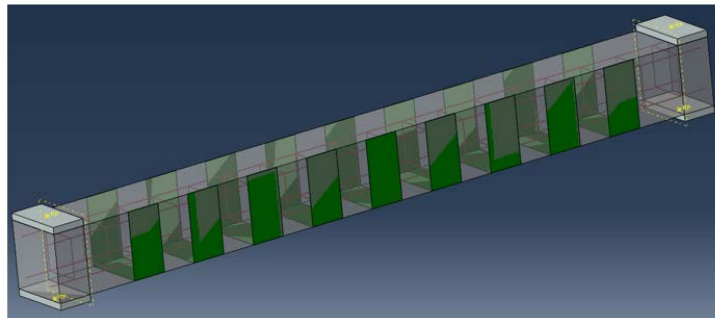


**Figure 10. Beam (B2) strengthened with U-Strip.**

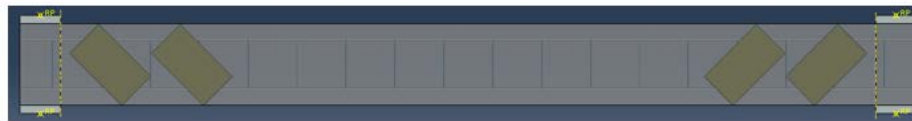


**Figure 11. Beam (B3) strengthened with diagonal strip.**

### 3. Results and Discussion

#### 3.1. Mid-Span deflection

It can be shown from Figure 12 that the beam strengthened with bottom strip “B1” had a less mid-span deflection than the unstrengthen beam “B0”, with a reduction percentage of 23 %. Similarly, the beam strengthened with U shape strip had a similar mid-span deflection value as beam B1, but with a less reduction percentage (around 21 %). These reductions are due to the high tensile strength of the CFRP sheets that helps in dissipating the energy from blast loading. These are similar to the findings reached by previous studies [17, 19]. On the other side, the beam strengthened with diagonal strips near supports (B3) experienced an increasing in the mid-span deflection as shown in Fig. 12. This is logical since diagonal strips will not affect the flexural behavior of RC beams; it is expected to affect the shear response of the beam. More details about mid-span deflection results are presented in Table 7.

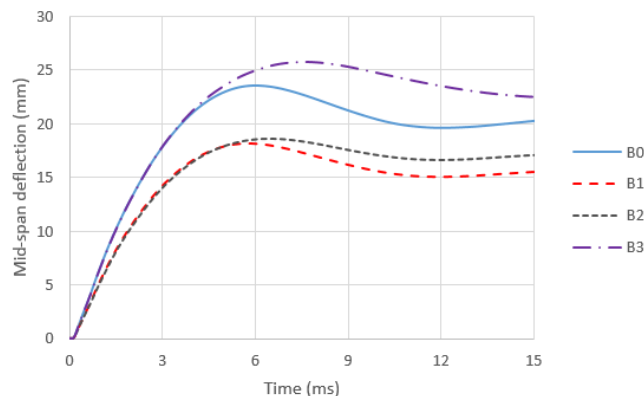


**Figure 12. Mid-Span deflection for all beams.**

### 3.2. Reinforcement strain

Using CFRP as strengthening techniques affects the strain in steel reinforcement depending on its position. For the beam strengthened with bottom strip "B1", it can be clearly seen from Fig. 13 that the strain in steel reinforcement was reduced. The reduction was about 16.6 % as shown in Table 7. Also for the beams strengthened with U-shape strip and diagonal strip a similar behavior realized (around 16.1 % reduction for "B2" and 18.2 % for "B3"). This is similar to the bottom rebar strain findings by [16, 23]. This is from the high tensile strength of the CFRP sheets that resist a part of the tensile stresses resulted from the blast load.

As for strain at compression steel the behavior is different. According to Fig. 14, the strain at compression reinforcement for the beam strengthened with bottom strips "B1" was increased by 65.8 %. This is because the strengthened section is resisting the blast load without failing, and that requires from it more resistance, which mean on other words more stresses at tension and compression. A similar behavior was realized for the beam strengthened with diagonal strips "B3", where the strain at compression reinforcement was increased by 30.5 %. The reason for this reduction is the same as for beam "B1" (the increasing in section strength). On the other side, beam "B2" that was strengthened with U-shape strips experienced a reduction in strain at compression reinforcement (around 60 %). This is due to the high confinement from the U-shape that makes the CFRP works at compression zone and drag some of the compression stresses from the compression reinforcement. More strain results are shown in Table 7.

Regarding strain at shear reinforcement, it can be concluded from Fig. 15 that both beams (B2) strengthened with U-shape strips and (B3) strengthened with diagonal strip experienced a reduction in strain at shear reinforcement stirrups near supports. This is due to the contribution of the U-shape and the diagonal CFRP sheets that have great contribution in resisting shear stress near supports. As for the beam strengthened with bottom strips (B1), the strain in shear reinforcement remains similar to that for the unstrengthen beam; since it works only in bottom tensile zone and had no contribution at shear zone near supports. Shear strain results for all beams are shown in Table 7.

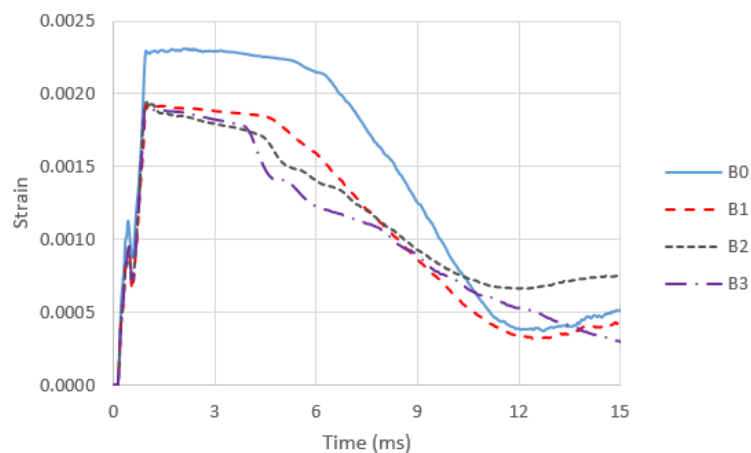


Figure 13. Tensile reinforcement strain.

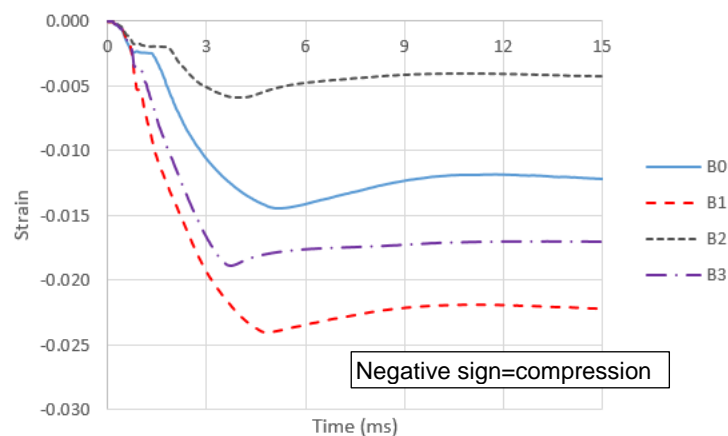


Figure 14. Compressive reinforcement strain.

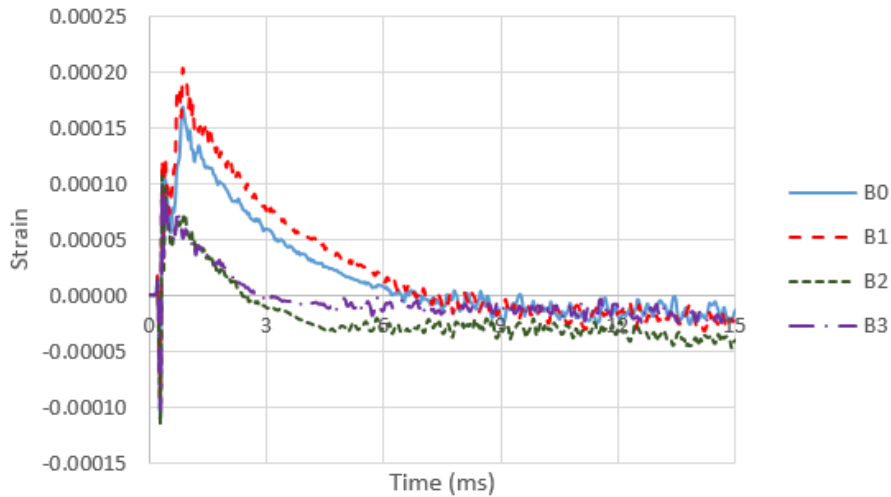


Figure 15. Shear reinforcement strain.

Table 7. Mid-span deflection, tensile strain, compressive strain, and shear strain results for all beams.

Beam	Mid-Span deflection "d" (mm)	Ratio ( $d_{1,2,3}/d_0$ )	Tensile reinforcement strain " $\epsilon_t$ "	Ratio ( $\epsilon_{t1,2,3} / \epsilon_{t0}$ )	Compressive reinforcement strain " $\epsilon_c$ "	Ratio ( $\epsilon_{c1,2,3} / \epsilon_{c0}$ )	Shear reinforcement strain " $\epsilon_s$ "	Ratio ( $\epsilon_{s1,2,3} / \epsilon_{s0}$ )
B0	23.5	-	0.00230	-	0.014	-	0.00017	-
B1	18.0	0.77	0.00192	0.83	0.023	1.66	0.00020	1.18
B2	18.5	0.79	0.00193	0.84	0.006	0.40	0.00011	0.65
B3	26.0	1.10	0.00188	0.82	0.019	1.35	0.00009	0.53

### 3.3. Structural damage

The tensile damage at bottom face for each beam is shown in Fig. 16 to 19. The un-strengthened beam experienced a tensile damaged zone with a width of 5.9 cm according to Fig. 6 and Table 5. This damage is due to plastic hinge formation at the middle of the beam and that may lead at some point to a total collapse of the beam due to un-stability. Although using CFRP in the beam with bottom strip "B1" has reduced the deflection and the strain at bottom steel reinforcement, it has increased the tensile damage at the bottom zone due to the shear failure between the CFRP sheet and the concrete bottom surface. As for the beams with U-shape strips "B2" and diagonal strips "B3", the tensile damage was not as concentrated as the beam "B1" since the CFRP surface was not fully attached to the concrete bottom surface. However, it still has less damage than the reference beam (two major cracks each has a width of nearly 1.5 cm).

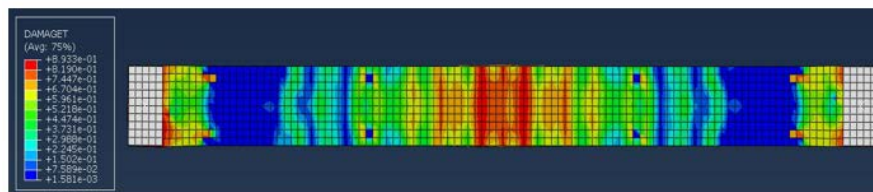


Figure 16. Bottom face damage for beam B0.

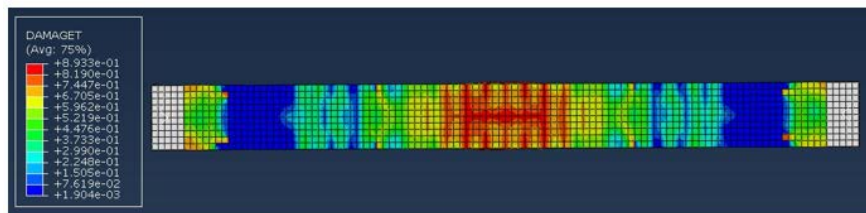


Figure 17. Bottom face damage for beam B1.

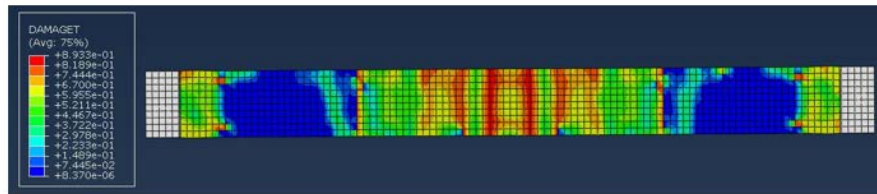


Figure 18. Bottom face damage for beam B2.

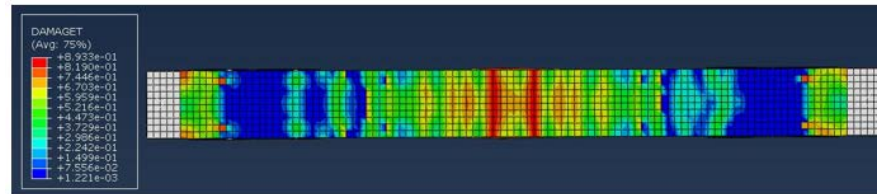


Figure 19. Bottom face damage for beam B3.

Fig. 20 to 23 show the compression damage in all beams. It can be seen that using CFRF sheets in deferent forms increased the compression damage at the beam top face. This is due to the bending resistance provided by the CFRP sheets that leads to a stress concentration in both tension and compression and as a results a more damage occurred at the top face. Both damage results (top and bottom) were similar to many previous researches [16, 17, 19, 23].

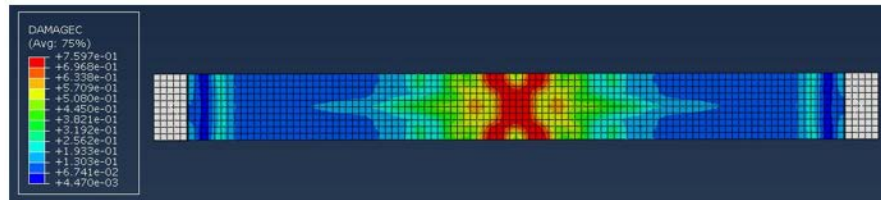


Figure 20. Top face damage for beam B0.

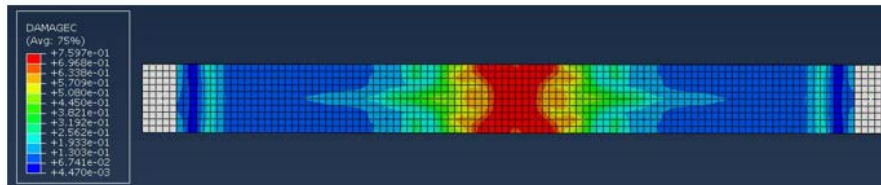


Figure 21. Top face damage for beam B1.

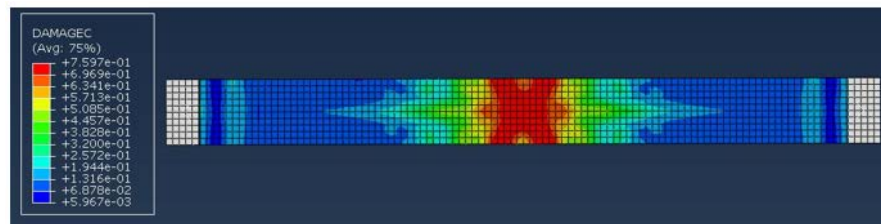


Figure 22. Top face damage for beam B2.

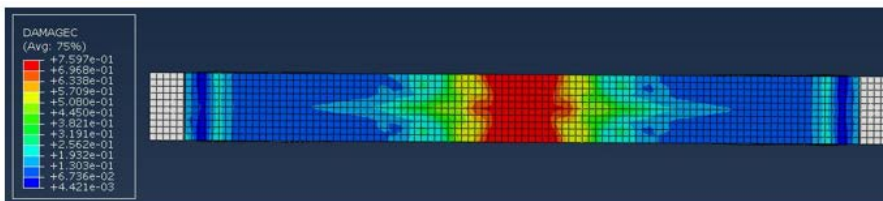


Figure 23. Top face damage for beam B3.

Tensile stresses in CFRP sheets are represented in Fig. 24 to 29. Fig. 24 shows the tensile stress in the CFRP used in the beam strengthened with bottom strip. The maximum stress was at the middle of the strip since the maximum moment was at the beam mid-span. It can be concluded that the CFRP did not

reach its tensile capacity. Fig. 25 shows the position of the maximum axial stress in the CFRP sheet. Similarly, the stresses in CFRP sheets in the strengthened beams with U-shape didn't reach the tensile capacity as shown in Figure 26 The critical strips lied at the mid-span of the strengthened beam as in Fig. 27. This also applies for the beam strengthened with diagonal strip where the critical strip lies near the support (Figure 28 and 29).

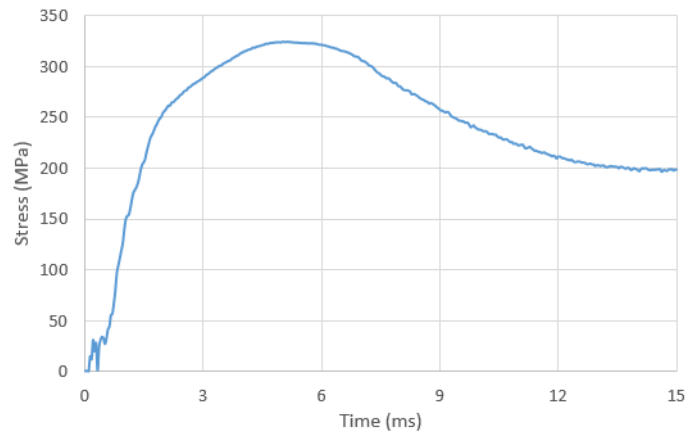


Figure 24. Tension stress in CFRP for beam B1.

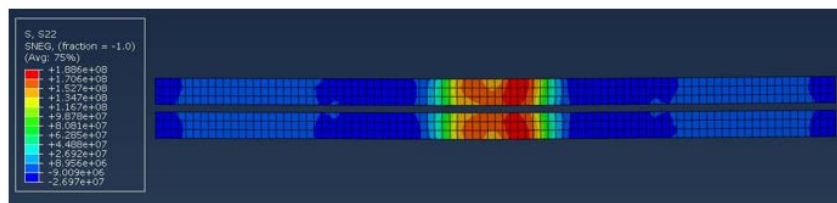


Figure 25. Position of maximum CFRP tension stress for beam B1.

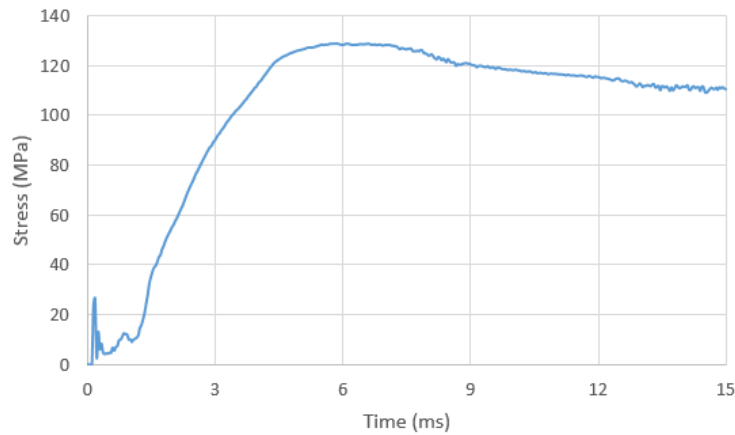


Figure 26. Tension stress in CFRP for beam B2.

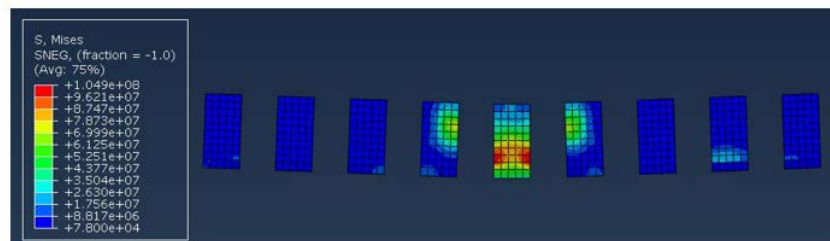
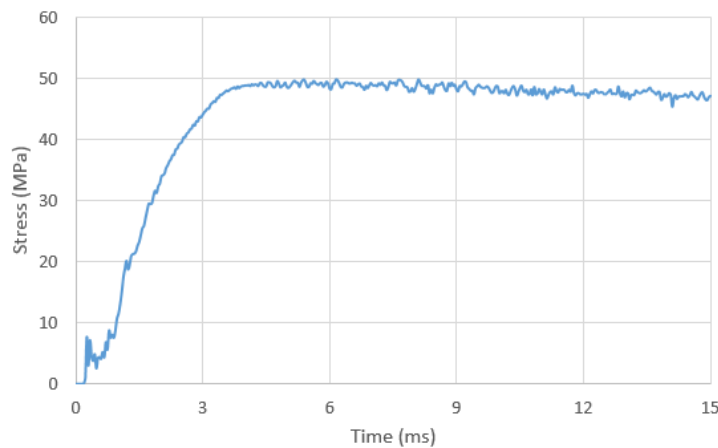
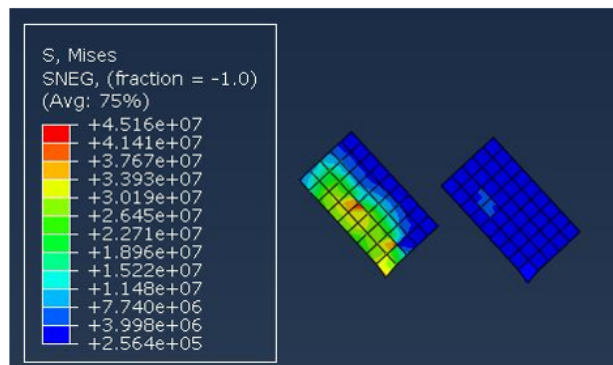


Figure 27. Position of maximum CFRP tension stress for beam B2.



**Figure 28. Tension stress in CFRP for beam B3.**



**Figure 29. Position of maximum CFRP tensile stress for beam B3.**

#### 4. Conclusion

The following conclusions can be made:

- Using CFRP in the bottom tensile face of RC beams helped in absorbing blast energy. This led to the reduction of the mid-span deflection for beams strengthened with bottom strips and U-shaped strips, with a better performance for the bottom strips (23 % reduction for bottom strips compared to 21 % for the U-shaped strips). As for the beam strengthened with diagonal strips this was not efficient as expected since the diagonal strips will act against shear stresses.
- Regarding steel reinforcement in tensile zone, using CFRP led to a reduction in the tensile strain in flexural reinforcement in all cases. The reduction was similar in all cases. On the other side, using CFRP in U-shapes was proved to confine the beam, which leads into a reduction in the compression steel strain too. This was not the case for beams with other strengthening techniques. As for shear reinforcement the best system was both diagonal and the U-shaped strips; since they both have vertical layers that resist the shear stresses. In contrast, the beam strengthened with bottom strips had no effect nearly on the shear reinforcement, which is logic too.
- Although using CFRP helped in dissipating blast energy, the beam strengthened with bottom strips (B1) has experienced more extensive tensile damage than the unstrengthen beam (B0). On the other side, both beams (B2) and (B3) that were strengthened with U-shaped and diagonal strips respectively had less tensile extensive damage than beams (B0) and (B1) due to the less contact area at the bottom face of the beam. As for compression damage at the top face of the beams, all strengthened beams (B1, B2, and B3) were damaged more than the reference beam (B0); since the CFRP laminates provide more confinement for the beam and hence more compression resistance were performed which led to the increased damage.
- There is no damage in any of the CFRP sheets since the maximum stresses inside each sheet did not reach their tensile capacity.

#### References

1. Temsah, Y., Jahami, A., Khatib, J., Sonebi, M. Numerical analysis of a reinforced concrete beam under blast loading. MATEC Web of Conferences. 2018. 149. Pp. 02063. DOI: 10.1051/mateconf/201814902063
2. Temsah, Y., Jahami, A., Khatib, J., Sonebi, M. Numerical Derivation of Iso-Damaged Curve for a Reinforced Concrete Beam Subjected to Blast Loading. MATEC Web of Conferences. 2018. 149. Pp. 02016. DOI: 10.1051/mateconf/201814902016

3. Jahami, A., Temsah, Y., Khatib, J. The efficiency of using CFRP as a strengthening technique for reinforced concrete beams subjected to blast loading. *International Journal of Advanced Structural Engineering*. 2019. 11(4). Pp. 411–420. DOI: 10.1007/s40091-019-00242-w
4. Cotsovos, D.M., Pavlović, M.N. Modelling of RC beams under impact loading. *Proceedings of the Institution of Civil Engineers: Structures and Buildings*. 2012. 165(2). Pp. 77–94. DOI: 10.1680/stbu.2012.165.2.77
5. Damasceno, I.I.R., Ferreira, M. de P., de Oliveira, D.R.C. Vigas de concreto armado sob cargas de impacto. *Acta Scientiarum – Technology*. 2014. 36(1). Pp. 23–31. DOI: 10.4025/actascitechnol.v36i1.17561
6. Rajput, A., Iqbal, M.A. Ballistic performance of plain, reinforced and pre-stressed concrete slabs under normal impact by an ogival-nosed projectile. *International Journal of Impact Engineering*. 2017. 110. Pp. 57–71. DOI: 10.1016/j.ijimpeng.2017.03.008.
7. Jahami, A., Temsah, Y., Khatib, J., Baalbaki, O., Darwiche, M., Chaaban, S. Impact behavior of rehabilitated post-tensioned slabs previously damaged by impact loading. *Magazine of Civil Engineering*. 2020. 93(1). Pp. 134–146. DOI: 10.18720/MCE.9-3.11.
8. Al Rawi, Y., Temsah, Y., Baalbaki, O., Jahami, A., Darwiche, M. Experimental investigation on the effect of impact loading on behavior of post-tensioned concrete slabs. *Journal of Building Engineering*. 2020. 31. Pp. 101207. DOI: 10.1016/j.job.2020.101207.
9. Mhanna, H.H., Hawileh, R.A., Abdalla, J.A. Shear strengthening of reinforced concrete beams using CFRP wraps. *Procedia Structural Integrity*. 2019. 17. Pp. 214–221. DOI: 10.1016/j.prostr.2019.08.029.
10. Michałowska-Maziejuk, D., Goszczyńska, B., Trąmpczyński, W. Effectiveness of strengthening pre-loaded RC beams with CFRP strips in conventional and accelerated strengthening procedures. *MATEC Web of Conferences*. 2019. 284. Pp. 06005. DOI: 10.1051/mateconf/201928406005
11. Naser, M.Z., Hawileh, R.A., Abdalla, J.A. Fiber-reinforced polymer composites in strengthening reinforced concrete structures: A critical review. *Engineering Structures*. 2019. 198(June). Pp. 109542. DOI: 10.1016/j.engstruct.2019.109542.
12. Yu, F., Zhou, H., Jiang, N., Fang, Y., Song, J., Feng, C., Guan, Y. Flexural experiment and capacity investigation of CFRP repaired RC beams under heavy pre-damaged level. *Construction and Building Materials*. 2020. 230. Pp. 117030. DOI: 10.1016/j.conbuildmat.2019.117030.
13. Yuan, X., Zhu, C., Zheng, W., Hu, J., Tang, B. Flexure Performance of Externally Bonded CFRP Plates-Strengthened Reinforced Concrete Members. *Mathematical Problems in Engineering*. 2020. 2020. DOI: 10.1155/2020/2604024
14. Kishore, R., Zia Nasiry, N., Muslim Rujhan, A. Strengthening of Reinforced Concrete Beams using CFRP laminates. *ASIAN JOURNAL OF CIVIL ENGINEERING (BHRC)*. 2016. 17(2). Pp. 159–167.
15. Osman, B.H., Wu, E., Ji, B., Abdulhameed, S.S. Effect of reinforcement ratios on shear behavior of concrete beams strengthened with CFRP sheets. *HBRC Journal*. 2018. 14(1). Pp. 29–36. DOI: 10.1016/j.hbrj.2016.04.002.
16. Bodzak, P. Flexural behaviour of concrete beams reinforced with different grade steel and strengthened by CFRP strips. *Composites Part B: Engineering*. 2019. 167(January). Pp. 411–421. DOI:10.1016/j.compositesb.2019.02.056.
17. Ali, M.I., Saleh, Y.A., Al Hasani, L.E., Khazaal, A.S., Abdulla, A.I. Behavior of RC Beams Strengthened by CFRP and Steel Rope under Frequent Impact Load. *Journal of advanced Sciences and Engineering Technologies*. 2018. 1(1). Pp. 30–42. DOI: 10.32441/jaset.v1i1.74
18. Pham, T.M., Chen, W., Elchalakani, M., Karrech, A., Hao, H. Experimental investigation on lightweight rubberized concrete beams strengthened with BFRP sheets subjected to impact loads. *Engineering Structures*. 2020. 205(December 2019). Pp. 110095. DOI: 10.1016/j.engstruct.2019.110095.
19. Wang, W., Chouw, N. Behaviour of CFRC beams strengthened by FFRP laminates under static and impact loadings. *Construction and Building Materials*. 2017. 155. Pp. 956–964. DOI: 10.1016/j.conbuildmat.2017.08.031.
20. Fujikake, K., Soeum, S., Matsui, T. CFRP strengthened RC beams subjected to impact loading. *Procedia Engineering*. 2017. 210. Pp. 173–181. DOI: 10.1016/j.proeng.2017.11.063.
21. Jahami, A., Temsah, Y., Khatib, J., Sonebi, M. NUMERICAL STUDY FOR THE EFFECT OF CARBON FIBER REINFORCED. *Symposium on Concrete Modelling (CONMOD2018)*. (August)Delft, Netherlands, 2018. Pp. 259–267.
22. Almusallam, T., Al-Salloum, Y., Alsayed, S., Iqbal, R., Abbas, H. Effect of CFRP strengthening on the response of RC slabs to hard projectile impact. *Nuclear Engineering and Design*. 2015. 286. Pp. 211–226. DOI: 10.1016/j.nucengdes.2015.02.017
23. Radnić, J., Matešan, D., Grgić, N., Baloević, G. Impact testing of RC slabs strengthened with CFRP strips. *Composite Structures*. 2015. 121. Pp. 90–103. DOI: 10.1016/j.compstruct.2014.10.033
24. Zhang, D., Yao, S.J., Lu, F., Chen, X.G., Lin, G., Wang, W., Lin, Y. Experimental study on scaling of RC beams under close-in blast loading. *Engineering Failure Analysis*. 2013. 33. Pp. 497–504. DOI: 10.1016/j.engfailanal.2013.06.020
25. Hibbitt, Karlsson, Sorensen. *ABAQUS User's Manual*, Pawtucket. 6<sup>th</sup> Edition. 2011.
26. Lubliner, J., Oliver, J., Oller, S., Onate, E. a Plastic-Damage Model. *International Journal of Solids and Structures*. 1989. 25(3). Pp. 299–326.
27. Lee, J., Fenves, G. Plastic-damage model for cyclic loading of concrete structure. *Engineering Mechanics*. 1998. 124(8). Pp. 892–900.

### **Contacts:**

*Ali Jahami, ahjahamy@hotmail.com*

*Yehya Temsah, ytemsah@bau.edu.lb*

*Jamal Khatib, j.khatib@bau.edu.lb*

*Ossama Baalbaki, obaalbaki@bau.edu.lb*

*Said Kenai, sdkenai@yahoo.com*